ELECTROELASTIC FIELDS INDUCED BY TWO COLLINEAR AND ENERGETICALLY CONSISTENT CRACKS IN A PIEZOELECTRIC LAYER

X.-C. Zhong

School of Mathematics and Information Science
Guangxi University
Nanning, Guangxi 530004, P.R. China

K.-Y. Lee *

State Key Laboratory of Structural Analysis for Industrial Equipment
Department of Engineering Mechanics
Dalian University of Technology
Dalian 116024, P.R. China

ABSTRACT

Within the framework of linear piezoelectricity, the problem of two collinear electrically dielectric cracks in a piezoelectric layer is investigated under inplane electro-mechanical loadings. The energetically consistent crack-face boundary conditions are utilized to address the effects of a dielectric inside the cracks on the crack growth. The Fourier transform technique is applied to solve the boundary-value problem. Under the consideration of two-case electromechanical loadings, the electroelastic fields near the inner and outer crack tips are obtained through the Lobatto-Chebyshev collocation method. The special case of two collinear energetically consistent cracks in an infinite piezoelectric solid is analyzed and the closed-form solutions of the crack-tip electroelastic fields are further determined. Numerical results show the variations of stress intensity factors and energy release rates near the inner and outer crack tips on the applied electric fields, the geometry of cracks and the width of the piezoelectric layer in graphics. The observations reveal that the stress intensity factors are dependent not only on the adopted crack-face boundary conditions, but also on the applied mechanical loading.

Keywords: Piezoelectric layer, Energetically consistent, Two collinear cracks, Fourier transform, Crack-tip fields.

1. INTRODUCTION

Due to the electromechanical coupling effects, many physical and mechanical problems of piezoelectric materials have attracted much attention [1-8]. One can see that the crack growth analysis of piezoelectric solids is complicated and dependent on many contributions such as the crack-tip inelastic deformation [9,10], the crack-tip domain switching [11] and the dielectric effects of crack interior [12-14]. From the experimental results [15], since the electric potential difference across the crack exists indeed, it can be also seen that the effects of the dielectric inside a crack on the crack growth should be considered.

For the crack-face boundary conditions, the permeable and impermeable ones are prevalent for a long time. Then Wang and Mai [16] have argued that the impermeable one is more reasonable than the permeable one in engineering problems. Moreover, to simulate the case of a crack with a dielectric interior, Hao and Shen [12] have proposed a semi-permeable crack-face electric boundary condition as follows

$$D^c = -\varepsilon^c \frac{\Delta\phi}{\Delta u_z}, \tag{1}$$

where $\varepsilon^c = \varepsilon_r \varepsilon_0$ ($\varepsilon_0 = 8.85 \times 10^{-12}$F/m) is the dielectric permittivity inside the crack. $\Delta\phi$ and Δu_z are the jumps of electric potential and crack opening displacement across the crack respectively. It has been applied widely to investigate the nonlinear fracture behavior for a cracked piezoelectric solid [1,17-21]. Furthermore, Landis and McMeeking [22] have firstly considered the electrostatic traction on the crack faces and analyzed the energy release rate of a half-infinite crack in a piezoelectric layer. Then Landis [13] has proposed the energetically consistent crack-face boundary conditions in the fracture mechanics of piezoelectric solids. That is, when a linear dielectric crack is considered, one has

$$D^c = -\varepsilon^c \frac{\Delta\phi}{\Delta u_z}, \quad \sigma^c = \frac{1}{2}\frac{(D^c)^2}{\varepsilon^c}, \tag{2}$$

* Corresponding author (KYL2813@gmail.com)

DOI : 10.1017/jmech.2014.31
Copyright © 2014 The Society of Theoretical and Applied Mechanics, R.O.C.
https://doi.org/10.1017/jmech.2014.31 Published online by Cambridge University Press

for $|D^c| \le \varepsilon^c E_d$. When the dielectric inside the cracks may be electrically breakdown, it follows that

$$sgn(D^c)E_d = -\frac{\Delta\phi}{\Delta u_z}, \quad D^c = -\varepsilon^c \frac{\Delta\phi}{\Delta u_z} + \omega_d ,$$
$$\sigma^c = E_d |\omega_d| + \frac{1}{2}\varepsilon^c E_d^2 , \tag{3}$$

for $|D^c| \ge \varepsilon^c E_d$. The constant E_d is defined as the critical electric field for corona discharges and ω_d stands for the amount of charge per unit area transferred between the crack faces. The energetically consistent crack-face boundary conditions are further verified by the finite element computation [23]. On the other hand, Ricoeur and Kuna [14] have also calculated the electrostatic traction acting on the crack faces and applied to solve the problem of a dielectric Griffith crack in a piezoelectric solid. Recently, Zhong and Zhang [24] have applied the energetically consistent crack-face boundary conditions to deal with the problem of a dielectric crack in a piezoelectric layer. Eskandari *et al*. [25] have made an electroelastic analysis of an energetically consistent annular crack in a piezoelectric solid. Using the self-consistent and the energetically consistent approaches, Fan *et al*. [26] have compared the observations for cracked piezoelectric ceramics. Zhong [27] has addressed the problem of an eccentric penny-shaped crack embedded in a piezoelectric layer by using the energetically consistent boundary conditions.

In the above-stated works, the energetically consistent boundary conditions are only used to solve the problems of a single crack in a piezoelectric solid. Owing to the interaction of multiple cracks, of much interest are the solutions of multi-cracks problems in a piezoelectric solid [28-30]. The objective of this paper is to investigate the interaction of two collinear energetically consistent cracks in a piezoelectric layer under two cases of electromechanical loadings. In order to solve the boundary-value problem, the Fourier transform technique is applied to obtain two coupling singular integral equations. The obtained equations are solved numerically through the Lobatto-Chebyshev collocation method and the electroelastic fields near the inner and outer crack tips are determined. The explicit solutions of two collinear energetically dielectric cracks in an infinite piezoelectric solid are given as a special case. Numerical computations for PZT-5H are carried out to show the variations of the stress intensity factors and the energy release rates in graphics on the applied electric field, the geometry of cracks and the width of the piezoelectric layer. The obtained results show that the inner crack tip is always easier to propagate than the outer crack tip regardless of the different mechanical loadings and crack-face boundary conditions.

2. STATEMENT OF THE PROBLEM

As shown in Fig. 1, it is assumed that a transversely isotropic piezoelectric layer is weakened by two collinear dielectric Griffith cracks. Here Cartesian

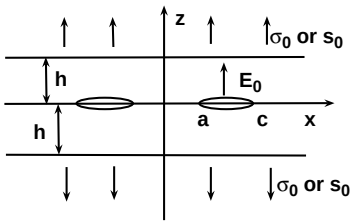


Fig. 1 Two collinear cracks embedded in a piezoelectric layer

coordinates system *xoz* is used and the poling axis is pointed to that as the *z*-axis. Two collinear cracks are situated at the segments of $a < |x| < c$ along the *x*-axis and the width of a piezoelectric layer is 2*h*. For a poled liner piezoelectric solid under the assumption of plane deformation, the constitutive equations can be read as

$$\sigma_{xx} = c_{11}s_{xx} + c_{13}s_{zz} - e_{31}E_z , \tag{4}$$

$$\sigma_{zz} = c_{13}s_{xx} + c_{33}s_{zz} - e_{33}E_z , \tag{5}$$

$$\sigma_{xz} = 2c_{44}s_{xz} - e_{15}E_x , \tag{6}$$

$$D_x = 2e_{15}s_{xz} + \varepsilon_{11}E_x , \tag{7}$$

$$D_z = e_{31}s_{xx} + e_{33}s_{zz} + \varepsilon_{33}E_z , \tag{8}$$

where σ_{ij} and s_{ij} are the components of stress and strain; D_i and E_i are the components of electric displacement and electric field, respectively; c_{kl}, ε_{kl} and e_{kl} are the elastic stiffness, the dielectric permittivities and piezoelectric constants, respectively.

On the other hand, it is convenient to express the components of strain and electric field through the non-vanishing elastic displacements $u_x(x, z)$ and $u_z(x, z)$ and the electric potential $\phi(x, z)$ as

$$s_{ij} = \frac{1}{2}(u_{i,j} + u_{j,i}), \quad E_i = -\phi_{,i} , \tag{9}$$

where a comma stands for partial differentiation with respect to the suffixed space variable, and *i*, *j* denote *x* and *z*. Moreover, application of the equations of equilibrium leads to the following basic governing equations

$$c_{11}u_{x,xx} + c_{44}u_{x,zz} + (c_{13} + c_{44})u_{z,xz} + (e_{31} + e_{15})\phi_{,xz} = 0 , \tag{10}$$

$$c_{44}u_{z,xx} + c_{33}u_{z,zz} + (c_{13} + c_{44})u_{x,xz} + e_{15}\phi_{,xx} + e_{33}\phi_{,zz} = 0 , \tag{11}$$

$$e_{15}u_{z,xx} + e_{33}u_{z,zz} + (e_{31} + e_{15})u_{x,xz} - \varepsilon_{11}\phi_{,xx} - \varepsilon_{33}\phi_{,zz} = 0 , \tag{12}$$

where the body forces and free charges have been neglected.

Now, to simulate two collinear cracks full of a dielectric, the energetically consistent crack-face boundary conditions are chosen. That is, we have

$$\sigma_{zz}(x,0) = \sigma^c , \quad D_z(x,0) = D^c , \quad a < |x| < c , \tag{13}$$

https://doi.org/10.1017/jmech.2014.31 Published online by Cambridge University Press

where σ^c and D^c are determined by the relations given in (2) or (3). Specially, $\varepsilon_r = 1$ implies that two collinear cracks are vacuum or full of air. In other words, it is found from (3) that when $-\Delta\phi/\Delta u_z > 0$, we have

$$E_d = -\frac{\Delta\phi}{\Delta u_z}, \quad D^c = \varepsilon^c E_d + \omega_d, \quad \sigma^c = E_d D^c - \frac{1}{2}\varepsilon^c E_d^2. \tag{14}$$

when $-\Delta\phi/\Delta u_z < 0$, it follows that

$$E_d = \frac{\Delta\phi}{\Delta u_z}, \quad D^c = -\varepsilon^c E_d + \omega_d, \quad \sigma^c = -E_d D^c - \frac{1}{2}\varepsilon^c E_d^2. \tag{15}$$

In the end, we consider two possible cases of applied electromechanical loadings, namely,

$$Case\ A: \sigma_{zz}(x,\pm h) = \sigma_0, \quad E_z(x,\pm h) = E_0, \tag{16}$$

$$Case\ B: s_{zz}(x,\pm h) = s_0, \quad E_z(x,\pm h) = E_0. \tag{17}$$

Case A means that the applied mechanical loading is stress. Case *B* implies that the applied mechanical loading is strain.

3. DERIVATION OF SINGULAR INTEGRAL EQUATIONS

Owing to the symmetry of the problem, it is sufficient to consider the electro-elastic field induced by two collinear dielectric cracks in the region $0 \le z < h$ and $0 < x < +\infty$. Then the free stress σ_{xz}, the elastic displacement $u_z(x, z)$ and the electric potential $\phi(x, z)$ satisfy

$$\sigma_{xz}(x,0) = 0, \quad 0 < x < +\infty, \tag{18}$$

$$u_z(x,0) = 0, \quad \phi(x,0) = 0, \quad 0 < x < a, c < x < +\infty. \tag{19}$$

In order to solve the partial differential Eqs. (10) ~ (12) with the boundary conditions (13), (16) ~ (19), the Fourier transform technique is feasible. Following Zhong and Zhang [24], the solutions of $u_z(x, z)$, $u_z(x, z)$ and $\phi(x, z)$ can be written as

$$u_x(x,z) = \sum_{j=1}^{3}\int_0^\infty A_j(\xi)\frac{\sinh\left[-\alpha_j\xi(z-h)\right]}{\cosh(\alpha_j\xi h)}\sin(\xi x)\,d\xi + B_1 x, \tag{20}$$

$$u_z(x,z) = \sum_{j=1}^{3}\eta_{3j}\,\alpha_j\int_0^\infty A_j(\xi)\frac{\cosh\left[-\alpha_j\xi(z-h)\right]}{\cosh(\alpha_j\xi h)}\cos(\xi x)d\xi + B_3 z, \tag{21}$$

$$\phi(x,z) = \sum_{j=1}^{3}\eta_{4j}\,\alpha_j\int_0^\infty A_j(\xi)\frac{\cosh\left[-\alpha_j\xi(z-h)\right]}{\cosh(\alpha_j\xi h)}\cos(\xi x)\,d\xi + B_4 z, \tag{22}$$

where $A_j(\xi)$ are the unknown functions to be solved and B_j are the constants to be determined by the boundary conditions. The constants α_j, η_{3j} and η_{4j} are given in Appendix A.

In what follows, from (4) ~ (8) and (20) ~ (22), it is easy to calculate the components of stress and electric displacement as

$$\begin{bmatrix}\sigma_{xx}(x,z)\\ \sigma_{zz}(x,z)\\ D_z(x,z)\end{bmatrix} = -\sum_{j=1}^{3}\begin{bmatrix}\beta_{0j}\\ \beta_{1j}\\ \beta_{2j}\end{bmatrix}\int_0^\infty \xi A_j(\xi)\frac{\sinh\left[-\alpha_j\xi(z-h)\right]}{\cosh(\alpha_j\xi h)}\cos(\xi x)\,d\xi + \begin{bmatrix}c_{11} & c_{13} & e_{31}\\ c_{13} & c_{33} & e_{33}\\ e_{31} & e_{33} & -\varepsilon_{33}\end{bmatrix}\begin{bmatrix}B_1\\ B_3\\ B_4\end{bmatrix}, \tag{23}$$

$$\begin{bmatrix}\sigma_{xz}(x,z)\\ D_x(x,z)\end{bmatrix} = -\sum_{j=1}^{3}\begin{bmatrix}\beta_{3j}\\ \beta_{4j}\end{bmatrix}\int_0^\infty \xi A_j(\xi)\frac{\cosh\left[-\alpha_j\xi(z-h)\right]}{\cosh(\alpha_j\xi h)}\sin(\xi x)\,d\xi, \tag{24}$$

where the constants $\beta_{kj}(k = 0, 1, 2, 3, 4)$ are given in Appendix A. Now it is necessary to give the values of the constants $\beta_j(j = 1, 3, 4)$. Under the applied electromechanical loadings, it is noted that one always uses the condition of zero shearing stress on the layer surfaces [31,32]. On the other hand, one also assumes that the material particles are constrained to move along the direction normal to the crack plane, which leads to the zero elastic displacement along the direction parallel to the crack plane when applied electromechanical loadings are acting on the crack surfaces [9,33,34]. Hence, when the applied electromechanical loadings are acting on the layer surfaces, we apply the boundary condition of $\sigma_{xx}(x, h) = 0$. Here it should be pointed out that generally some amount of bending in the layers will create and the condition of $\sigma_{xx}(x, h) = 0$ will make the results be in slightly error compared with the accurate solution for a small *h* especially. But this treatment can make our calculations easy and the obtained results significant. Then application of (18) and (19) , we have

$$Case\ A: \begin{bmatrix}B_1\\ B_3\\ B_4\end{bmatrix} = \begin{bmatrix}c_{11} & c_{13} & e_{31}\\ c_{13} & c_{33} & e_{33}\\ 0 & 0 & -1\end{bmatrix}^{-1}\begin{bmatrix}0\\ \sigma_0\\ E_0\end{bmatrix}, \tag{25}$$

$$Case\ B: \begin{bmatrix}B_1\\ B_3\\ B_4\end{bmatrix} = \begin{bmatrix}c_{11} & c_{13} & e_{31}\\ 0 & 1 & 0\\ 0 & 0 & -1\end{bmatrix}^{-1}\begin{bmatrix}0\\ s_0\\ E_0\end{bmatrix}. \tag{26}$$

Hereafter "–1" denotes the corresponding inverse matrix.

Now, let us focus on the solutions of the unknown functions $A_j(\xi)(j = 1, 2, 3)$. From (18) and (24), one has

https://doi.org/10.1017/jmech.2014.31 Published online by Cambridge University Press

$$\sum_{j=1}^{3}\beta_{3j}\,A_j(\xi)=0\,. \tag{27}$$

On the other hand, application of the boundary conditions (13) and (19) leads to two coupling dual integral equations, namely

$$\sum_{j=1}^{3}\begin{bmatrix}\eta_{3j}\\ \eta_{4j}\end{bmatrix}\int_0^\infty \alpha_j A_j(\xi)\cos(\xi x)\,d\xi=\begin{bmatrix}0\\0\end{bmatrix},\quad 0<x<a\,,\quad x>c\,, \tag{28}$$

$$\sum_{j=1}^{3}\begin{bmatrix}\beta_{1j}\\ \beta_{2j}\end{bmatrix}\int_0^\infty \xi A_j(\xi)\tanh(\alpha_j\xi h)\cos(\xi x)\,d\xi=\begin{bmatrix}\sigma_h-\sigma^c\\ D_h-D^c\end{bmatrix},\quad a<x<c\,, \tag{29}$$

where

$$Case\ A:\begin{bmatrix}\sigma_h\\ D_h\end{bmatrix}=\begin{bmatrix}c_{13} & c_{33} & e_{33}\\ e_{31} & e_{33} & -\varepsilon_{33}\end{bmatrix}\begin{bmatrix}c_{11} & c_{13} & e_{31}\\ c_{13} & c_{33} & e_{33}\\ 0 & 0 & -1\end{bmatrix}^{-1}\begin{bmatrix}0\\ \sigma_0\\ E_0\end{bmatrix}, \tag{30}$$

$$Case\ B:\begin{bmatrix}\sigma_h\\ D_h\end{bmatrix}=\begin{bmatrix}c_{13} & c_{33} & e_{33}\\ e_{31} & e_{33} & -\varepsilon_{33}\end{bmatrix}\begin{bmatrix}c_{11} & c_{13} & e_{31}\\ 0 & 1 & 0\\ 0 & 0 & -1\end{bmatrix}^{-1}\begin{bmatrix}0\\ s_0\\ E_0\end{bmatrix}. \tag{31}$$

Furthermore, we introduce the following auxiliary functions

$$\begin{bmatrix}\Psi_1(x)\\ \Psi_2(x)\end{bmatrix}=\frac{\partial}{\partial x}\begin{bmatrix}u_z(x,0)\\ \phi(x,0)\end{bmatrix}. \tag{32}$$

Then the unknowns $A_j(\xi)$ can be determined as

$$\begin{bmatrix}A_1(\xi)\\ A_2(\xi)\\ A_3(\xi)\end{bmatrix}=-\frac{2}{\pi\xi}\cdot[b_{ji}]_{3\times3}\int_a^c\begin{bmatrix}\Psi_1(s)\\ \Psi_2(s)\\ 0\end{bmatrix}\sin(s\xi)\,ds\,, \tag{33}$$

with

$$[b_{ji}]_{3\times3}=\begin{bmatrix}\eta_{31}\alpha_1 & \eta_{32}\alpha_2 & \eta_{33}\alpha_3\\ \eta_{41}\alpha_1 & \eta_{42}\alpha_2 & \eta_{43}\alpha_3\\ \beta_{31} & \beta_{32} & \beta_{33}\end{bmatrix}^{-1}. \tag{34}$$

Let us substitute (33) into (29) and obtain two coupling integral equations:

$$\frac{2}{\pi}\sum_{i=1}^{2}\sum_{j=1}^{3}b_{ji}\begin{bmatrix}\beta_{1j}\\ \beta_{2j}\end{bmatrix}\int_a^c\int_0^\infty \Psi_i(s)\tanh(\alpha_j\xi h)\sin(s\xi)\cos(x\xi)\,d\xi ds=-\begin{bmatrix}\sigma_h-\sigma^c\\ D_h-D^c\end{bmatrix}, \tag{35}$$

for $a<x<c$. Then recalling the known result [36]

$$\int_0^\infty\frac{\tanh(\alpha_j h\xi)\cos(t\xi)}{\xi}\,d\xi=\ln\left|\coth\left(\frac{t\pi}{4\alpha_j h}\right)\right|, \tag{36}$$

one has

$$\int_0^\infty\tanh(\alpha_j h\xi)\sin(s\xi)\cos(x\xi)\,d\xi=\frac{1}{2}\frac{d}{dx}\ln\left|\frac{\sinh\left(\frac{\pi}{2h\alpha_j}x\right)+\sinh\left(\frac{\pi}{2h\alpha_j}s\right)}{\sinh\left(\frac{\pi}{2h\alpha_j}x\right)-\sinh\left(\frac{\pi}{2h\alpha_j}s\right)}\right|. \tag{37}$$

In the end the singular integral equations can be derived. That is, we have

$$\frac{1}{\pi}\sum_{i=1}^{2}\sum_{j=1}^{3}b_{ji}\begin{bmatrix}\beta_{1j}\\ \beta_{2j}\end{bmatrix}\int_a^c\Psi_i(s)\frac{\pi}{h\alpha_j}\frac{\cosh\left(\frac{\pi}{2h\alpha_j}x\right)\sinh\left(\frac{\pi}{2h\alpha_j}s\right)}{\sinh^2\left(\frac{\pi}{2h\alpha_j}s\right)-\sinh^2\left(\frac{\pi}{2h\alpha_j}x\right)}ds=-\begin{bmatrix}\sigma_h-\sigma^c\\ D_h-D^c\end{bmatrix}, \tag{38}$$

for $a<x<c$.

4. SOLUTIONS OF SINGULAR INTEGRAL EQUATIONS

4.1 The Limiting Case

Generally speaking, we can not obtain the explicit solutions of the singular integral Eq. (38) for the complexity of the kernels. However, when $h\to+\infty$, meaning that two collinear energetically consistent cracks are embedded in an infinite piezoelectric solid, Eqs. (38) become very simple. It is expedient to give the closed-form solutions of the electroelastic fields near the inner and outer crack tips. For the special case of $h\to+\infty$, it is found that

$$\lim_{h\to+\infty}\frac{\pi}{h\alpha_j}\frac{\cosh\left(\frac{\pi}{2h\alpha_j}x\right)\sinh\left(\frac{\pi}{2h\alpha_j}s\right)}{\sinh^2\left(\frac{\pi}{2h\alpha_j}s\right)-\sinh^2\left(\frac{\pi}{2h\alpha_j}x\right)}=\frac{2s}{s^2-x^2}. \tag{39}$$

Then Eqs. (38) can be rewritten as

$$\frac{1}{\pi}\int_a^c\frac{2s}{s^2-x^2}\begin{bmatrix}\Psi_1(s)\\ \Psi_2(s)\end{bmatrix}ds=-\begin{bmatrix}x_{11} & x_{12}\\ x_{21} & x_{22}\end{bmatrix}^{-1}\begin{bmatrix}\sigma_h-\sigma^c\\ D_h-D^c\end{bmatrix}, \tag{40}$$

with

$$x_{ki}=\sum_{j=1}^{3}b_{ij}\beta_{kj}\,,\quad k,i=1,2\,. \tag{41}$$

https://doi.org/10.1017/jmech.2014.31 Published online by Cambridge University Press

In what follows, it is attempt to obtain the explicit solutions of Eqs. (40). If introducing the following variable transformations:

$$\bar{s} = s^2\,,\quad \bar{x} = x^2\,,\quad \bar{a} = a^2\,,\quad \bar{c} = c^2\,,\quad \Psi_i(s) = \bar{\Psi}_i(\bar{s})\,. \tag{42}$$

Equation (40) can be reread as

$$\frac{1}{\pi}\int_{\bar{a}}^{\bar{c}} \frac{1}{\bar{s}-\bar{x}}\begin{bmatrix}\bar{\Psi}_1(\bar{s})\\ \bar{\Psi}_2(\bar{s})\end{bmatrix} d\bar{s} = -\begin{bmatrix}x_{11} & x_{12}\\ x_{21} & x_{22}\end{bmatrix}^{-1}\begin{bmatrix}\sigma_h-\sigma^c\\ D_h-D^c\end{bmatrix}. \tag{43}$$

The obtained relations (43) are the standard singular integral equations with Cauchy kernel and the explicit solutions are given as

$$\begin{bmatrix}\bar{\Psi}_1(\bar{s})\\ \bar{\Psi}_2(\bar{s})\end{bmatrix} = -\begin{bmatrix}x_{11} & x_{12}\\ x_{21} & x_{22}\end{bmatrix}^{-1}\begin{bmatrix}\sigma_h-\sigma^c\\ D_h-D^c\end{bmatrix}\frac{1}{\pi\sqrt{(\bar{x}-\bar{a})(\bar{c}-\bar{x})}} \cdot\int_{\bar{a}}^{\bar{c}}\frac{\sqrt{(\bar{s}-\bar{a})(\bar{c}-\bar{s})}}{\bar{x}-\bar{s}}\,d\bar{s} \quad + \frac{1}{\sqrt{(\bar{x}-\bar{a})(\bar{c}-\bar{x})}}\begin{bmatrix}C_1\\ C_2\end{bmatrix}, \tag{44}$$

where $C_i\,(i=1,\ 2)$ are the constants which can be determined by

$$\int_a^c \Psi_i(s)\,ds = 0\,, \tag{45}$$

or in terms of the introduced variables

$$\int_{\bar{a}}^{\bar{c}} \frac{\bar{\Psi}_i(\bar{s})}{2\sqrt{\bar{s}}}\,d\bar{s} = 0\,. \tag{46}$$

Substituting (44) into (46), we have

$$\begin{bmatrix}C_1\\ C_2\end{bmatrix} = -\begin{bmatrix}x_{11} & x_{12}\\ x_{21} & x_{22}\end{bmatrix}^{-1}\begin{bmatrix}\sigma_h-\sigma^c\\ D_h-D^c\end{bmatrix}\begin{bmatrix}\dfrac{\bar{a}+\bar{c}}{2}-\dfrac{\bar{c}E(k)}{F(k)}\end{bmatrix}, \tag{47}$$

where $F(\cdot)$ and $E(\cdot)$ are the complete elliptic integrals of the first and second kind respectively and hereafter $k=\sqrt{(\bar{c}-\bar{a})/\bar{c}}$. Furthermore, the solutions of $\bar{\Psi}_i(\bar{x})(i=1,2)$ can be given as

$$\begin{bmatrix}\bar{\Psi}_1(\bar{x})\\ \bar{\Psi}_2(\bar{x})\end{bmatrix} = -\begin{bmatrix}x_{11} & x_{12}\\ x_{21} & x_{22}\end{bmatrix}^{-1}\begin{bmatrix}\sigma_h-\sigma^c\\ D_h-D^c\end{bmatrix}\frac{1}{\sqrt{(\bar{x}-\bar{a})(\bar{c}-\bar{x})}}\begin{bmatrix}\bar{x}-\dfrac{\bar{c}E(k)}{F(k)}\end{bmatrix}. \tag{48}$$

From the above results, it is found that the solutions of $\bar{\Psi}_i(\bar{x})(i=1,2)$ are expressed as the explicit forms for the case of two collinear energetically consistent cracks in an infinite piezoelectric solid. Furthermore, the closed-form solutions for the case of a Griffith crack in an infinite piezoelectric solid should be reduced from Eqs. (48). It is noted that

$$E(k)=\int_0^{\pi/2}\sqrt{1-k^2\sin^2\theta}\,d\theta\,,\quad F(k)=\int_0^{\pi/2}\frac{1}{\sqrt{1-k^2\sin^2\theta}}\,d\theta\,. \tag{49}$$

If letting $a\to 0$, meaning that two collinear cracks is reduced to a crack with the length of $2c$, we obtain $k=1$ and $E(k)/F(k)\to 0$, then

$$\begin{bmatrix}\bar{\Psi}_1(\bar{x})\\ \bar{\Psi}_2(\bar{x})\end{bmatrix} = -\begin{bmatrix}x_{11} & x_{12}\\ x_{21} & x_{22}\end{bmatrix}^{-1}\begin{bmatrix}\sigma_h-\sigma^c\\ D_h-D^c\end{bmatrix}\sqrt{\frac{\bar{x}}{\bar{c}-\bar{x}}}\,. \tag{50}$$

4.2 The General Case

For the case of two collinear energetically consistent cracks embedded in a piezoelectric layer with a finite width, the numerical solutions of Eqs. (38) will be given. In order to carry out the numerical computations, we introduce the variable transformations as follows:

$$x = a_0\hat{x}+c_0\,,\quad s = a_0\hat{s}+c_0\,,\quad \Psi_i(s)=\hat{\Psi}_i(\hat{s})\,, \tag{51}$$

where $a_0=(c-a)/2$, $c_0=(c+a)/2$ and $-1<\hat{x}<1$. Then Eqs. (38) can be rewritten as

$$\frac{1}{\pi}\sum_{i=1}^{2}\sum_{j=1}^{3}b_{ji}\begin{bmatrix}\beta_{1j}\\ \beta_{2j}\end{bmatrix}\int_{-1}^{1}\hat{\Psi}_i(\hat{s})\frac{a_0\pi}{h\alpha_j}\frac{\cosh\left(\dfrac{a_0\hat{x}+c_0}{2h\alpha_j}\pi\right)\sinh\left(\dfrac{a_0\hat{s}+c_0}{2h\alpha_j}\pi\right)}{\sinh^2\left(\dfrac{a_0\hat{s}+c_0}{2h\alpha_j}\pi\right)-\sinh^2\left(\dfrac{a_0\hat{x}+c_0}{2h\alpha_j}\pi\right)}d\hat{s} = -\begin{bmatrix}\sigma_h-\sigma^c\\ D_h-D^c\end{bmatrix}. \tag{52}$$

From the viewpoint of the fracture mechanics, it is assumed that the functions $\hat{\Psi}_i(\hat{s})$ exhibit the inverse square-root singularity, namely

$$\hat{\Psi}_i(\hat{s}) = \frac{\Theta_i(\hat{s})}{\sqrt{1-\hat{s}^2}}\,, \tag{53}$$

where $\Theta_i(\hat{s})$ are bounded continuous functions in the interval $|\hat{s}|\le 1$. Noting that

$$\lim_{s\to x}\left[\frac{\pi}{h\alpha_j}\frac{\cosh\left(\dfrac{\pi}{2h\alpha_j}x\right)\sinh\left(\dfrac{\pi}{2h\alpha_j}s\right)}{\sinh^2\left(\dfrac{\pi}{2h\alpha_j}s\right)-\sinh^2\left(\dfrac{\pi}{2h\alpha_j}x\right)}-\frac{1}{s-x}\right] = \frac{\pi}{2h\alpha_j}\sinh^{-1}\frac{\pi}{2h\alpha_j}x\,, \tag{54}$$

and using the Lobatto-Chebyshev collocation method, we obtain a system of algebraic equations as follows

$$\frac{1}{n}\sum_{l=0}^{n}\lambda_l\frac{1}{\hat{s}_l-\hat{x}_m}\sum_{i=1}^{2}\begin{bmatrix}x_{1i}\\ x_{2i}\end{bmatrix}\Theta_i(\hat{s}_l) + \frac{1}{n}\sum_{l=0}^{n}\lambda_l\sum_{i=1}^{2}\begin{bmatrix}Y_{1i}(\hat{s}_l,\hat{x}_m)\\ Y_{2i}(\hat{s}_l,\hat{x}_m)\end{bmatrix}\Theta_i(\hat{s}_l) = -\begin{bmatrix}\sigma_h-\sigma^c\\ D_h-D^c\end{bmatrix}, \tag{55}$$

https://doi.org/10.1017/jmech.2014.31 Published online by Cambridge University Press

where

$$\begin{bmatrix} Y_{1i}(\hat{s}_l, \hat{x}_m) \\ Y_{2i}(\hat{s}_l, \hat{x}_m) \end{bmatrix} = \sum_{j=1}^{3} b_{ji} \begin{bmatrix} \beta_{1j} \\ \beta_{2j} \end{bmatrix} \frac{a_0 \pi}{h\alpha_j} \cdot \frac{\cosh\left(\frac{a_0 \hat{x}_m + c_0}{2h\alpha_j}\pi\right) \sinh\left(\frac{a_0 \hat{s}_l + c_0}{2h\alpha_j}\pi\right)}{\sinh^2\left(\frac{a_0 \hat{s}_l + c_0}{2h\alpha_j}\pi\right) - \sinh^2\left(\frac{a_0 \hat{x}_m + c_0}{2h\alpha_j}\pi\right)} - \frac{1}{\hat{s}_l - \hat{x}_m} \quad (56)$$

with

$$\hat{x}_m = \cos\left[(2m-1)\pi/(2n)\right], \quad m = 1, 2, \cdots, n, \quad (57)$$

$$\hat{s}_l = \cos(l\pi/n), \quad l = 0, 1, 2, \cdots, n, \quad (58)$$

$$\lambda_0 = \lambda_n = 1/2, \quad \lambda_1 = \cdots = \lambda_{n-1} = 1. \quad (59)$$

On the other hand, application of (45) and (53) yields

$$\int_{-1}^{1} \frac{\Theta_i(\hat{s})}{\sqrt{1-\hat{s}^2}} d\hat{s} = 0, \quad i = 1, 2, \quad (60)$$

which can be further rewritten as

$$\sum_{l=0}^{n} \lambda_l \Theta_i(\hat{s}_l) = 0, \quad i = 1, 2. \quad (61)$$

Now Eqs. (55) and (61) form a system of algebraic equations, which can be solved directly under the condition that D_c and σ^c are known. One can see that the Lobatto-Chebyshev collocation method is convergent for $n \to \infty$ and it is more accurate than the Gauss-Chebyshev numerical integration method [35].

5. CRACK TIP FIELDS

In this section, of much interest are the crack-tip electroelastic fields induced by two collinear cracks. For the inner and outer crack tips, here we define the intensity factors of stress and electric displacement as

$$\begin{bmatrix} K_\sigma^{inn} \\ K_D^{inn} \end{bmatrix} = \lim_{x \to a^-} \sqrt{2\pi(a-x)} \begin{bmatrix} \sigma_{zz}(x, 0) \\ D_z(x, 0) \end{bmatrix}, \quad (62)$$

$$\begin{bmatrix} K_\sigma^{out} \\ K_D^{out} \end{bmatrix} = \lim_{x \to c^+} \sqrt{2\pi(x-c)} \begin{bmatrix} \sigma_{zz}(x, 0) \\ D_z(x, 0) \end{bmatrix}, \quad (63)$$

and the intensity factors of crack opening displacement and electric potential as

$$\begin{bmatrix} K_{COD}^{inn} \\ K_\phi^{inn} \end{bmatrix} = \lim_{x \to a^+} \sqrt{\frac{\pi}{2(x-a)}} \begin{bmatrix} u_z(x, 0) \\ \phi(x, 0) \end{bmatrix}, \quad (64)$$

$$\begin{bmatrix} K_{COD}^{out} \\ K_\phi^{out} \end{bmatrix} = \lim_{x \to c^-} \sqrt{\frac{\pi}{2(c-x)}} \begin{bmatrix} u_z(x, 0) \\ \phi(x, 0) \end{bmatrix}. \quad (65)$$

Moreover, if defining the energy release rates as

$$G^{inn} = \lim_{\delta \to 0} \frac{1}{\delta} \int_0^\delta \left[\sigma_{zz}(a-x, 0)\, u_z(a-x+\delta, 0) + D_z(a-x, 0)\phi(a-x+\delta, 0)\right] dx, \quad (66)$$

$$G^{out} = \lim_{\delta \to 0} \frac{1}{\delta} \int_0^\delta \left[\sigma_{zz}(x+c, 0)\, u_z(x+c-\delta, 0) + D_z(x+c, 0)\, \phi(x+c-\delta, 0)\right] dx, \quad (67)$$

where δ ($\delta << (c-a)$) is the distance of the crack tip advancing, we have

$$G^{inn} = \frac{1}{2}(K_\sigma^{inn} K_{COD}^{inn} + K_D^{inn} K_\phi^{inn}), \quad (68)$$

$$G^{out} = \frac{1}{2}(K_\sigma^{out} K_{COD}^{out} + K_D^{out} K_\phi^{out}). \quad (69)$$

Note that D^c and σ^c are two unknown constants which should be determined firstly. In what follows, we give the solutions of D^c and σ^c for the limiting case of $h \to +\infty$ and the general case, then the intensity factors of stress, electric displacement, crack opening displacement and electric potential near the inner and outer crack tips respectively.

5.1 The Limiting Case

For the limiting case of $h \to +\infty$, the jumps of elastic displacement and electric potential can be calculated explicitly. According to (32), one has

$$\begin{bmatrix} \Delta u_z(x, 0) \\ \Delta\phi(x, 0) \end{bmatrix} = 2\int_a^x \begin{bmatrix} \Psi_1(s) \\ \Psi_2(s) \end{bmatrix} ds, \quad a < x < c, \quad (70)$$

with the knowledge of (48), we arrive at

$$\begin{bmatrix} \Delta u_z(x, 0) \\ \Delta\phi(x, 0) \end{bmatrix} = -2c \left[\frac{E(k)}{F(k)} F(\theta, k) - E(\theta, k)\right] \begin{bmatrix} x_{11} & x_{12} \\ x_{21} & x_{22} \end{bmatrix}^{-1} \begin{bmatrix} \sigma_h - \sigma^c \\ D_h - D^c \end{bmatrix}, \quad (71)$$

where $F(\theta, k)$ and $E(\theta, k)$ are the incomplete elliptical integrals of the first and second kinds respectively, with

$$\theta = \arcsin\sqrt{\frac{c^2 - x^2}{c^2 - a^2}}. \quad (72)$$

Application of (2) leads to

$$[D^c \quad \varepsilon^c] \begin{bmatrix} x_{11} & x_{12} \\ x_{21} & x_{22} \end{bmatrix}^{-1} \begin{bmatrix} \sigma_h - \sigma^c \\ D_h - D^c \end{bmatrix} = 0, \quad (73)$$

for $|D^c| \le \varepsilon^c E_d$. Equation (73) is a cubic equation with respect to D^c, which is identical to the known results [13,14,25]. It is also seen from (73) that D^c is dependent on the material properties, the permeability of the dielectric inside the cracks and applied

https://doi.org/10.1017/jmech.2014.31 Published online by Cambridge University Press

electromechanical loadings. The geometry of two cracks can not affect the value of D^c. These phenomena are in accordance with those given by Landis [13] and Eskandari *et al*. [25]. Moreover, when D^c is obtained, σ^c can be determined through the second relation in (2). On the other hand, for $|D^c| \geq \varepsilon^c E_d$ and $-\Delta\phi/\Delta u_z > 0$, it follows that

$$[E_d \quad 1]\begin{bmatrix} x_{11} & x_{12} \\ x_{21} & x_{22} \end{bmatrix}^{-1}\begin{bmatrix} \sigma_h - E_d D^c + \varepsilon^c E_d^2/2 \\ D_h - D^c \end{bmatrix} = 0\,, \tag{74}$$

when $|D^c| \geq \varepsilon^c E_d$ and $-\Delta\phi/\Delta u_z < 0$, we have

$$[E_d \quad -1]\begin{bmatrix} x_{11} & x_{12} \\ x_{21} & x_{22} \end{bmatrix}^{-1}\begin{bmatrix} \sigma_h + E_d D^c + \varepsilon^c E_d^2/2 \\ D_h - D^c \end{bmatrix} = 0\,. \tag{75}$$

According to (74) or (75), D^c can be obtained for a given discharge field E_d. Then the second equation in (14) or (15) is used to determine σ^c.

Once D^c and σ^c are determined, the intensity factors together with the energy release rates can be obtained. Making use of (23), (48), (62) ~ (65) and (71), after some computations, we obtain

$$\begin{bmatrix} K_\sigma^{inn} \\ K_D^{inn} \end{bmatrix} = -\frac{\sqrt{\pi}}{\sqrt{a(c^2-a^2)}}\begin{bmatrix} a^2 - \dfrac{c^2 E(k)}{F(k)} \end{bmatrix}\begin{bmatrix} \sigma_h - \sigma^c \\ D_h - D^c \end{bmatrix}, \tag{76}$$

$$\begin{bmatrix} K_\sigma^{out} \\ K_D^{out} \end{bmatrix} = \frac{\sqrt{\pi}}{\sqrt{c(c^2-a^2)}}\begin{bmatrix} c^2 - \dfrac{c^2 E(k)}{F(k)} \end{bmatrix}\begin{bmatrix} \sigma_h - \sigma^c \\ D_h - D^c \end{bmatrix}, \tag{77}$$

and

$$\begin{bmatrix} K_{COD}^{inn} \\ K_\phi^{inn} \end{bmatrix} = c\begin{bmatrix} \dfrac{cE(k)}{aF(k)} - \dfrac{a}{c} \end{bmatrix}\sqrt{\frac{\pi a}{c^2-a^2}}\begin{bmatrix} x_{11} & x_{12} \\ x_{21} & x_{22} \end{bmatrix}^{-1}\begin{bmatrix} \sigma_h - \sigma^c \\ D_h - D^c \end{bmatrix}, \tag{78}$$

$$\begin{bmatrix} K_{COD}^{out} \\ K_\phi^{out} \end{bmatrix} = -c\begin{bmatrix} \dfrac{E(k)}{F(k)} - 1 \end{bmatrix}\sqrt{\frac{\pi c}{c^2-a^2}}\begin{bmatrix} x_{11} & x_{12} \\ x_{21} & x_{22} \end{bmatrix}^{-1}\begin{bmatrix} \sigma_h - \sigma^c \\ D_h - D^c \end{bmatrix}. \tag{79}$$

Additionally, it is noted that using the semi-permeable crack-face boundary conditions, Hao [29] has obtained the closed-form solutions of two collinear cracks in a piezoelectric solid through reducing the crack problem to a Riemann-Hilbert problem. The obtained stress intensity factors in (76) and (77) are in agreement with those given by Hao [29] except for the factor $\sigma_h - \sigma^c$ and here the Fourier transform technique is applied.

5.2 The General Case

Generally, when $|D^c| \leq \varepsilon^c E_d$, it is seen from (2) that

$$D^c \int_x^c \Psi_1(s)\,ds + \varepsilon^c \int_x^c \Psi_2(s)\,ds = 0\,, \quad a < x < c\,, \tag{80}$$

or

$$D^c \int_{\hat{x}}^1 \frac{\Theta_1(\hat{s})}{\sqrt{1-\hat{s}^2}}\,d\hat{s} + \varepsilon^c \int_{\hat{x}}^1 \frac{\Theta_2(\hat{s})}{\sqrt{1-\hat{s}^2}}\,d\hat{s} = 0\,, \quad -1 < \hat{x} < 1\,, \tag{81}$$

where the relations (51) and (53) have been used. Eq. (81) is an Abel integral equation, which is solved by using the Lobatto-Chebyshev quadrature technique in Zhong and Zhang [24]. That is, for $\hat{x} = 0$ one has

$$D^c \sum_{l=0}^{n/2} \lambda_l \Theta_1(\hat{s}_l) + \varepsilon^c \sum_{l=0}^{n/2} \lambda_l \Theta_2(\hat{s}_l) = 0\,, \tag{82}$$

where n is chosen as an even number. Obviously, Eqs. (55), (61) and (82) form a nonlinear system with $2n + 3$ unknowns, which can be solved as those given in Zhong and Zhang [24] and the detail procedures are omitted here.

In addition, when $|D^c| \geq \varepsilon^c E_d$ and $-\Delta\phi/\Delta u_z > 0$, one arrives at

$$E_d \sum_{l=0}^{n/2} \lambda_l \Theta_1(\hat{s}_l) + \sum_{l=0}^{n/2} \lambda_l \Theta_2(\hat{s}_l) = 0\,. \tag{83}$$

when $|D^c| \geq \varepsilon^c E_d$ and $-\Delta\phi/\Delta u_z < 0$, it is found that

$$E_d \sum_{l=0}^{n/2} \lambda_l \Theta_1(\hat{s}_l) - \sum_{l=0}^{n/2} \lambda_l \Theta_2(\hat{s}_l) = 0\,. \tag{84}$$

Making use of Eqs. (55), (61) along with (83) or (84), similar to Zhong and Zhang [24], we can determine the solution of D^c, then give σ^c by using the second equation in (14) or (15).

In what follows, we focus on the intensity factors of stress and electric displacement. From (23), the components of stress and electric displacement can be computed as

$$\begin{bmatrix} \sigma_{zz}(x,0) \\ D_z(x,0) \end{bmatrix} = \frac{1}{\pi}\sum_{i=1}^{2}\sum_{j=1}^{3} b_{ji}\begin{bmatrix} \beta_{1j} \\ \beta_{2j} \end{bmatrix}\int_a^c \Psi_i(s)\frac{\pi}{h\alpha_j} \frac{\cosh\left(\dfrac{\pi}{2h\alpha_j}x\right)\sinh\left(\dfrac{\pi}{2h\alpha_j}s\right)}{\sinh^2\left(\dfrac{\pi}{2h\alpha_j}s\right) - \sinh^2\left(\dfrac{\pi}{2h\alpha_j}x\right)}\,ds + \begin{bmatrix} \sigma_h \\ D_h \end{bmatrix}, \tag{85}$$

for $0 < x < a$ and $x > c$. Under the consideration of (54), one can get

$$\begin{bmatrix} \sigma_{zz}(x,0) \\ D_z(x,0) \end{bmatrix} = \frac{1}{\pi}\sum_{i=1}^{2}\sum_{j=1}^{3} b_{ji}\begin{bmatrix} \beta_{1j} \\ \beta_{2j} \end{bmatrix}\int_a^c \frac{\Psi_i(s)}{s-x}\,ds + O(1)\,. \tag{86}$$

Application of (51), (53), (62) and (63) leads to

$$\begin{bmatrix} K_\sigma^{inn} \\ K_D^{inn} \end{bmatrix} = \sqrt{\pi a_0}\begin{bmatrix} x_{11} & x_{12} \\ x_{21} & x_{22} \end{bmatrix}\begin{bmatrix} \Theta_1(-1) \\ \Theta_2(-1) \end{bmatrix}, \tag{87}$$

$$\begin{bmatrix} K_\sigma^{out} \\ K_D^{out} \end{bmatrix} = -\sqrt{\pi a_0}\begin{bmatrix} x_{11} & x_{12} \\ x_{21} & x_{22} \end{bmatrix}\begin{bmatrix} \Theta_1(1) \\ \Theta_2(1) \end{bmatrix}. \tag{88}$$

Similarly, the intensity factors of crack opening displacement and electric potential can be determined as

https://doi.org/10.1017/jmech.2014.31 Published online by Cambridge University Press

$$\begin{bmatrix} K_{COD}^{inn} \\ K_{\phi}^{inn} \end{bmatrix} = \sqrt{\pi a_0} \begin{bmatrix} \Theta_1(-1) \\ \Theta_2(-1) \end{bmatrix}, \tag{89}$$

$$\begin{bmatrix} K_{COD}^{out} \\ K_{\phi}^{out} \end{bmatrix} = -\sqrt{\pi a_0} \begin{bmatrix} \Theta_1(1) \\ \Theta_2(1) \end{bmatrix}. \tag{90}$$

The energy release rates near the inner and outer crack tips can be obtained easily by using (68) and (69) respectively.

6. NUMERICAL RESULTS AND DISCUSSION

In this section, we investigate the variations of the stress intensity factors and the energy release rates near the inner and outer crack tips respectively. In the following computations the piezoelectric material PZT-5H is chosen (Table 1) and the case of two collinear vacuum cracks (*i.e.* ε_r = 1) in a piezoelectric layer is only considered for the sake of simplicity. The applied mechanical loadings are σ_0 = 10 MPa for Case A and s_0c_{33} = 10 MPa for Case B respectively.

First, we compare the effects of applied electric fields on the stress intensity factors by using the semi-permeable and the energetically consistent crack-face boundary conditions respectively. For convenience, the limiting case of two collinear linear cracks in an infinite piezoelectric solid is considered. Under the electromechanical loading $E_0 / \sigma_0 = 0.02$ (m^2/C), Fig. 2 shows the variations of the normalized stress intensity factor $K_\sigma / \sigma_0(\pi a_0)^{1/2}$ on the ratio a_0 / c_0 for Case A. Using the semi-permeable crack-face boundary conditions, one can see from Fig. 2 that the applied electric field has no influences on the stress intensity factors, which is in agreement with the known results (see, *e.g.*, Hao [29]; Li and Lee [21]). However, applying the energetically consistent boundary conditions, it is found that the applied electric field decreases the stress intensity factors, which is in accordance with those given in Ricoeur and Kuna [14] and Zhong and Zhang [24]. In addition, of much interest are the effects of the geometry of two collinear cracks on the stress intensity factors. One can see from Fig. 2 that with increasing a_0 / c_0, the stress intensity factors near the inner and outer crack tips are increasing regardless of the adopted crack-face boundary conditions. It implies that the smaller the distance between two collinear cracks, the greater the interactions of two collinear cracks are. Specially, when $a_0 / c_0 \to 0$ (*i.e.*, $c_0 \to \infty$), the stress intensity factor near the inner crack tip is identical to that near the outer crack tip. That is, with the increasing of the distance of two collinear cracks, the stress intensity factors are tending to that corresponding to a piezoelectric solid with a crack [21]. As usual, for a fixed $0 < a_0 / c_0 < 1$, the stress intensity factor near the inner crack tip is greater than that near the outer crack tip for two cases of crack-face boundary conditions respectively, meaning that the inner crack tip is easier to propagate than the outer crack tip. On the other hand,

Table 1 The relevant material properties

PZT-5H	c_{11}	c_{33}	c_{13}	c_{44}	e_{31}	e_{33}	e_{15}	ε_{11}	ε_{33}
	126	117	53	35.3	–6.5	23.3	17	15.1	13.0

Units: elastic stiffness constant, GPa; piezoelectric constants, C/m^2; dielectric permittivities, ($\times 10^{-9}$)C^2/Nm^2

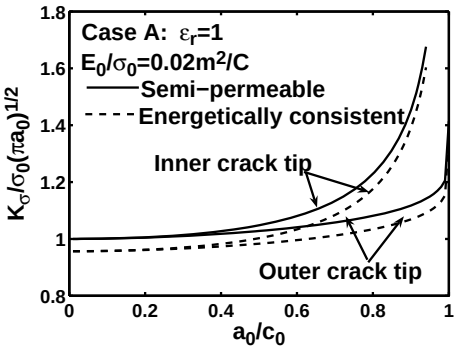


Fig. 2 The variations of $K_\sigma / \sigma_0\sqrt{\pi a_0}$ on a_0 / c_0 for two collinear linear cracks in an infinite piezoelectric solid and Case A

under the assumption of Case *B* and the electromechanical loadings E_0 / s_0c_{33} = –0.01, 0, 0.01 (m^2/C), the normalized stress intensity factors K_σ / s_0c_{33} $(\pi a_0)^{1/2}$ versus the ratio a_0 / c_0 are depicted in Fig. 3 using the semi-permeable crack-face boundary conditions and Fig. 4 using the energetically consistent boundary conditions, respectively. The comparison between Figs. 3 and 4 reveal that the applied positive electric loading always decreases the stress intensity factors and the applied negative one always increase the stress intensity factor. It means that a positive electric loading impedes the crack growth and a negative one enhances the crack growth for two cases of crack-face boundary conditions. The above phenomenon agrees well with that given by Kumar and Singh [37] through the finite element technique for a cracked piezoelectric solid under a strain loading. From Figs. 3 and 4, it is also found that the effects of applied electric fields on the stress intensity factors are strong dependent on the applied mechanical loading. And the values of stress intensity factors using the semi-permeable boundary conditions are more than those using the energetically consistent boundary conditions for $E_0 \neq 0$ and a fixed a_0 / c_0, which is in agreement with that in Fig. 2. In addition, one can see that in Figs. 2, 3 and 4, the values for the inner crack tip are given for a smaller range of a_0 / c_0 than those for the outer crack tip. It is attributed to the reason that when $a_0 / c_0 \to 1$, the distance between two collinear cracks will tend to zero and the values of the physics quantities for the inner crack tip will tend to infinity. Specially, it is interesting to give the values of stress intensity factors near the outer crack tip for $a_0 / c_0 \to 1$. In Fig. 2, one can obtain $K_\sigma / \sigma_0(\pi a_0)^{1/2} \approx 1.414$ for a semi-permeable crack and $K_\sigma / \sigma_0(\pi a_0)^{1/2} \approx 1.353$ for an energetically

https://doi.org/10.1017/jmech.2014.31 Published online by Cambridge University Press

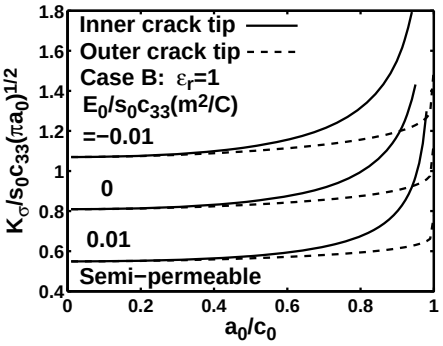


Fig. 3 The variations of $K_\sigma / \sigma_0\sqrt{\pi a_0}$ on a_0 / c_0 for two collinear linear cracks in an infinite piezoelectric solid and Case B using the semi-permeable boundary conditions

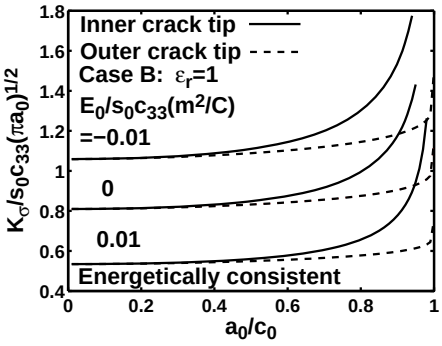


Fig. 4 The variations of $K_\sigma / \sigma_0\sqrt{\pi a_0}$ on a_0 / c_0 for two collinear linear cracks in an infinite piezoelectric solid and Case B using the energetically consistent boundary conditions

consistent crack. In Fig. 3, it follows that K_σ / s_0c_{33} $(\pi a_0)^{1/2} \approx 1.513, 1.145, 0.7766$ for $E_0 / s_0c_{33} = -0.01, 0, 0.01$ (m^2/C) respectively. In Fig. 4, we can have K_σ / s_0c_{33} $(\pi a_0)^{1/2} \approx 1.498, 1.145, 0.7555$ for $E_0 / s_0c_{33} = -0.01, 0, 0.01$ (m^2/C) respectively.

Second, it is interesting to investigate the influences of the discharge field E_d on the stress intensity factors and the energy release rates, respectively. For comparisons, here we consider that two collinear energetically consistent cracks are embedded in an infinite piezoelectric solid under the assumption of Case *A*. For $\varepsilon_r = 1$ and $a_0 / c_0 = 0.5$, Figs. 5 and 6 are drawn to show the variations of the normalized stress intensity factor $K_\sigma / \sigma_0(\pi a_0)^{1/2}$ and the normalized energy release rate G/G_0 versus E_d with the electromechanical loadings of $E_0 / \sigma_0 = 0.02, -0.02$ (m^2/C) respectively, where G_0 denotes the energy release rate of a permeable crack in a piezoelectric solid [21]. From Figs. 5 and 6, one can see that when $E_d \to 0$, corresponding to the case of two collinear permeable cracks in a piezoelectric solid, the curves of $E_0 / \sigma_0 = 0.02$ (m^2/C) and those of $E_0 / \sigma_0 = -0.02$ (m^2/C) are overlapping. The observations show again that the applied electric loadings have no influences on the stress intensity factor and the energy release rate for a permeable crack in a piezoelectric solid [3]. Furthermore, when E_d is rising, the stress intensity factors near the inner and outer crack tips are decreasing, then a little increasing. Generally, It is seen from Figs. 2 and 5 that applied electric loadings decrease the stress intensity factor for Case *A*. On the other hand, as shown in Fig. 6, the energy release rates are dropping down with an increasing E_d, which is in agreement with the observations given in Landis [13] and Eskandari *et al*. [25]. Contrary to those in Fig. 6, Fig. 5 shows that the stress intensity factors are increasing when E_d is greater than 2.5 (MV/cm). The phenomenon is due to the fact that when $E_d > 2.5$ (MV/cm), the electrostatic traction acting on the crack surface will decrease. In addition, it should be pointed out that one has $E_d \le 3.1$ MV/cm for $E_0 / \sigma_0 = 0.02$ m^2/C and $E_d \le 3.15$ MV/cm for $E_0 / \sigma_0 = -0.02$ m^2/C to satisfy the condition $| D^c | \ge \varepsilon^c E_d$.

In the end, we focus on the width effects of a piezoelectric layer on the stress intensity factors. For simplicity, we only consider the case of a piezoelectric layer with two collinear linear cracks. In the numerical computiions, the Lobatto-Chebyshev collocation method will be used. In order to get a good approximation, one can find that it is enough to choose $n = 30$ after carring out a series of numerical examples. The variations of the stress intensity factors on the ratio a_0 / c_0 are shown in Figs. 7 and 8 for Cases A and B with $c_0 / h = 1.2, 1.0, 0.8$ respectively. For a fixed $a_0 / c_0 \ne 0$, the stress intensity factors near the inner and outer crack tips are rising with an increasing c_0 / h for Cases *A* and *B*, which is similar to those for two collinear cracks in a purely elastic layer [38]. The above phenomenon reveals that two collinear cracks embedded in a piezoelectric layer are easier to grow than those in an infinite piezoelectric solid.

7. CONCLUSIONS

Under the assumption of the energetically consistent crack-face boundary conditions, the problem of two collinear dielectric cracks in a piezoelectric layer is considered for two cases of electromechanical loadings. The Fourier transform technique is used to solve the boundary-value problem and two dual integral equations are derived, then two singular integral equations with Cauchy kernel are given. For the case of an infinite piezoelectric solid with two collinear cracks, the derived singular integral equations are solved explicitly. For the general case of a piezoelectric layer with two collinear cracks, numerical solutions are constructed. The intensity factors of stress, electric displacement, COD and electric potential and the energy release rates are further calculated. The main observations are given as follows:

- The stress intensity factor is dependent not only on the adopted crack-face boundary conditions, but also on the applied mechanical loadings.
- Based on the stress intensity factor, two collinear cracks in a piezoelectric layer are easier to propagate than those in an infinite piezoelectric solid.

https://doi.org/10.1017/jmech.2014.31 Published online by Cambridge University Press

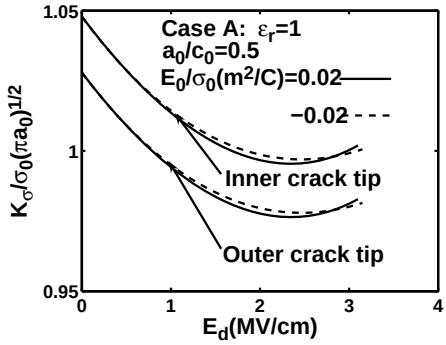


Fig. 5 The variations of $K_\sigma / \sigma_0 \sqrt{\pi a_0}$ on E_d for two collinear cracks in an infinite piezoelectric solid

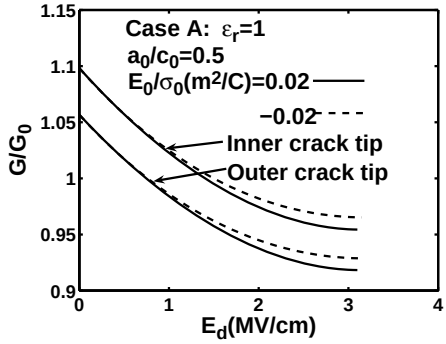


Fig. 6 The variations of G/G_0 on E_d for two collinear cracks in an infinite piezoelectric solid

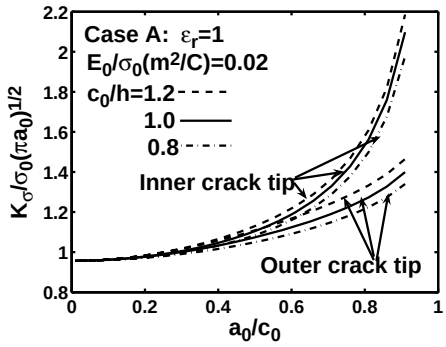


Fig. 7 The variations of $K_\sigma / \sigma_0 \sqrt{\pi a_0}$ on a_0 / c_0 for two collinear linear cracks in an piezoelectric layer and Case A

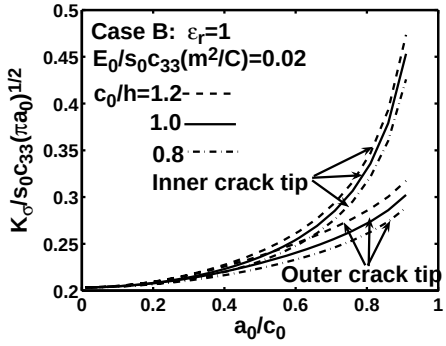


Fig. 8 The variations of $K_\sigma / \sigma_0 \sqrt{\pi a_0}$ on a_0 / c_0 for two collinear linear cracks in an piezoelectric layer and Case B

- With an increase of the discharge field E_d, the energy release rates near the inner and outer crack tips are decreasing.
- The inner crack tip is always easier to growth than the outer one regardless of the crack-face boundary conditions and the applied mechanical loadings.

ACKNOWLEDGEMENTS

The authors would like to thank the anonymous referee for the valuable comments and suggestions for improving the paper. The work was supported by the National Natural Science Foundation of China (No: 11362002).

APPENDIX A

The constants α_j (j = 1, 2, 3) (Re [α_j] > 0) can be obtained by solving the following characteristic equation

$$\begin{vmatrix} c_{11}-c_{44}\alpha^2 & -(c_{13}+c_{44})\,\alpha & -(e_{31}+e_{15})\,\alpha \\ -(c_{13}+c_{44})\,\alpha & c_{33}\alpha^2-c_{44} & e_{33}\alpha^2-e_{15} \\ -(e_{31}+e_{15})\,\alpha & e_{33}\alpha^2-e_{15} & \varepsilon_{11}-\varepsilon_{33}\alpha^2 \end{vmatrix} = 0\,. \quad \text{(A1)}$$

Then η_{3j} and η_{4j} are determined through

$$\begin{aligned} \alpha_j^2 &= \frac{c_{11}}{c_{44}+(c_{13}+c_{44})\,\eta_{3j}+(e_{31}+e_{15})\,\eta_{4j}} \\ &= \frac{c_{13}+c_{44}+c_{44}\eta_{3j}+e_{15}\eta_{4j}}{c_{33}\eta_{3j}+e_{33}\eta_{4j}} \\ &= \frac{e_{31}+e_{15}+e_{15}\eta_{3j}-\varepsilon_{11}\eta_{4j}}{e_{33}\eta_{3j}-\varepsilon_{33}\eta_{4j}}\,. \end{aligned} \quad \text{(A2)}$$

The constants β_{kj}(k = 1, 2, 3, 4) are given as

$$\beta_{0j} = (c_{13}\eta_{3j}+e_{31}\eta_{4j})\,\alpha_j^2 - c_{11}\,, \quad \text{(A3)}$$

$$\beta_{1j} = (c_{33}\eta_{3j}+e_{33}\eta_{4j})\,\alpha_j^2 - c_{13}\,, \quad \text{(A4)}$$

$$\beta_{2j} = (e_{33}\eta_{3j}-\varepsilon_{33}\eta_{4j})\,\alpha_j^2 - e_{31}\,, \quad \text{(A5)}$$

$$\beta_{3j} = \left[c_{44}(1+\eta_{3j})+e_{15}\eta_{4j}\right]\alpha_j\,, \quad \text{(A6)}$$

$$\beta_{4j} = \left[e_{15}(1+\eta_{3j})-\varepsilon_{11}\eta_{4j}\right]\alpha_j\,. \quad \text{(A7)}$$

REFERENCES

1. McMeeking, R. M., “Crack Tip Energy Release Rate for a Piezoelectric Compact Tension Specimen,” *Engineering Fracture Mechanics*, **64**, pp. 217–244 (1999).

https://doi.org/10.1017/jmech.2014.31 Published online by Cambridge University Press

2. Yang, W., *Mechatronic Reliability*, Tsinghua University Press/Springer, Beijing (2001).
3 .Qin, Q. H., *Fracture Mechanics of Piezoelectric Materials*, WIT Press, Southampton (2001).
4. Ding, H. J., Wang, H. M. and Chen, W. Q., "Analytical Solution of a Special Non-Homogeneous Pyroelectric Hollow Cylinder for Piezothermoelastic Axisymmetric Plane Strain Dynamic Problems," *Applied Mathematics and Computation*, **151**, pp. 423–441 (2004).
5. Zhang, T. Y. and Gao, C. F., "Fracture Behaviors of Piezoelectric Materials," *Theoretical and Applied Fracture Mechanics*, **41**, pp. 339–379 (2004).
6. Barboteu, M. and Sofonea, M., "Solvability of a Dynamic Contact Problem Between a Piezoelectric Body and a Conductive Foundation," *Applied Mathematics and Computation*, **215**, pp. 2978–2991 (2009).
7. Kuna, M., "Fracture Mechanics of Piezoelectric Materials -Where are We Right Now?" *Engineering Fracture Mechanics*, **77**, pp. 309–326 (2010).
8. Guo, J. H., Lu, Z. X., Han, H. T. and Yang, Z. Y., "The Behavior of Two Non-Symmetrical Permeable Crack Semanating from an Elliptical Hole in a Piezoelectric Solid," *European Journal of Mechanics A/Solids*, **29**, pp. 654–663 (2010).
9. Gao, H., Zhang, T. Y. and Tong, P., "Local and Global Energy Release Rate for an Electrically Yielded Crack in a Piezoelectric Ceramic," *Journal of the Mechanics and Physics of Solids*, **45**, pp. 491–510 (1997).
10. Zhang, T. Y., Zhao, M. H. and Gao, C. F., "The Strip Dielectric Breakdown Model," *International Journal of Fracture*, **132**, pp. 311–327 (2005).
11. Zhu, T. and Yang, W., "Toughness Variation of Ferroelectrics by Polarization Switch Under Nonuniform Electric Field," *Acta Materialia*, **45**, pp. 4695–4702 (1997).
12. Hao, T. H. and Shen, Z. Y., "A New Electric Boundary Condition of Electric Fracture Mechanics and Its Application," *Engineering Fracture Mechanics*, **47**, pp. 793–802 (1994).
13. Landis, C. M., "Energetically Consistent Boundary Conditions for Electromechanical Fracture," *International Journal of Solids and Structures*, **41**, pp. 6291–6315 (2004).
14. Ricoeur, A. and Kuna, M., "Electrostatic Tractions at Crack Faces and Their Influence on the Fracture Mechanics of Piezoelectrics," *International Journal of Fracture*, **157**, pp. 3–12 (2009).
15. Schneider, G. A., Felten, F. and McMeeking, R. M., "The Electrical Potential Difference Across Cracks in PZT Measured by Kelvin Probe Microscopy and Implications for Fracture," *Acta Materialia*, **51**, pp. 2235–2241 (2003).
16. Wang, B. L. and Mai, Y. W., "Impermeable Crack and Permeable Crack Assumptions, which One is More Realistic?" *Journal of Applied Mechanics*, ASME, **71**, pp. 575–578 (2007).
17. Wang, X. D. and Jiang, L. Y., "The Effective Electroelastic Property of Piezoelectric Media with Parallel Dielectric Cracks," *International Journal of Solids and Structures*, **40**, pp. 5287–5303 (2003).
18. Wang, X. D. and Jiang, L. Y., "The Nonlinear Fracture Behavior of an Arbitrarily Oriented Dielectric Crack in Piezoelectric Materials," *Acta Mechanica*, **172**, pp. 195–210 (2004).
19. Wang, X. D. and Jiang, L. Y., "Coupled Behaviour of Interacting Dielectric Cracks in Piezoelectric Materials," *International Journal of Fracture*, **132**, pp. 115–133 (2005).
20. Chiang, C. R. and Weng, G. J., "Nonlinear Behavior and Critical State of a Penny-Shaped Dielectric Crack in a Piezoelectric Solid," *Journal of Applied Mechanics*, ASME, **74**, pp. 852–860 (2007).
21. Li, X. F. and Lee, K. Y., "Fracture Analysis of Cracked Piezoelectric Materials," *International Journal of Solids and Structures*, **41**, pp. 4137–4161 (2004).
22. Landis, C. M. and McMeeking, R. M., "Modeling of Fracture in Ferroelectric Ceramics," *Proceeding of SPIE*, **3992**, pp. 176–184 (2000).
23. Li, W., McMeeking, R. M. and Landis, C. M., "On the Crack Face Boundary Conditions in Electromechanical Fracture and an Experimental Protocol for Determining Energy Release Rate," *European Journal of Mechanics A/Solids*, **27**, pp. 285–301 (2008).
24. Zhong, X. C. and Zhang, K. S., "Electroelastic Analysis of an Electrically Dielectric Griffith Crack in a Piezoelectric Layer," *International Journal of Engineering Science*, **48**, pp. 612–623 (2010).
25. Eskandari, M., Moeini-Ardakani, S. S. and Shodja, H. M., "An Energetically Consistent Annular Crack in a Piezoelectric Medium," *Engineering Fracture Mechanics*, **77**, pp. 819–831 (2010).
26. Fan, C. Y., Zhao, M. H., Meng, L. C., Gao, C. F. and Zhang, T. Y., "On The Self-Consistent, Energetically Consistent, and Electrostatic Traction Approaches in Piezoelectric Fracture Mechanics," *Engineering Fracture Mechanics*, **78**, pp. 2338–2355 (2011).
27. Zhong, X. C., "Fracture Analysis of a Piezoelectric Layer with a Penny-Shaped and Energetically Consistent Crack," *Acta Mechanica*, **223**, pp. 331–345 (2012).
28. Zhang, T. Y. and Hack, J. E., "Mode-III Crack in Piezoelectric Materials," *Journal of Applied Physics*, **71**, pp. 58–65 (1992).
29. Hao, T. H., "Multiple Collinear Cracks in a Piezoelectric Material," *International Journal of Solids and Structures*, **38**, pp. 9201–9208 (2001).
30. Liu, F. and Zhong, X. C., "Transient Response of Two Collinear Dielectric Cracks in a Piezoelectric Solid Under Inplane Impacts," *Applied Mathematics and Computation*, **217**, pp. 3779–3791 (2010).
31. Wang, X. Y. and Yu, S. W., "Transient Response of a Crack in Piezoelectric Strip Subjected to the Mechanical and Electrical Impacts: Mode-I Problem,"

https://doi.org/10.1017/jmech.2014.31 Published online by Cambridge University Press

Mechanics of Materials, **33**, pp. 11–22 (2001).
32. Wang, B. L., Nod, N., Han, J. C. and Du, S. Y., "A Penny-Shaped Crack in a Transversely Isotropic Piezoelectric Layer," *European Journal of Mechanics of A/Solids*, **20**, pp. 997–1005 (2001).
33. Rice, J. M., Ben-Zion, Y. and Kim, K. S., "Three-Dimensional Perturbation Solution for a Dynamic Planar Crack Moving Unsteadily in a Model Elastic Solid," *Journal of the Mechanics and Physics of Solids*, **42**, pp. 813–843 (1994).
34. Li, X. F. and Lee, K. Y., "Effects of Electric Field on Crack Growth for a Penny-Shaped Dielectric Crack in a Piezoelectric Layer," *Journal of the Mechanics and Physics of Solids*, **52**, pp. 2079–2100 (2004).
35. Theocaris, P. S. and Ioakimidis, N. I., "Numerical Integration Methods for the Solution of Singular Integral Equations," *Quarterly of Applied Mathematics*, **35**, pp. 173–185 (1977).
36. Gradshteyn, I. S. and Ryzhik, I. M., *Table of Integrals, Series and Products*, Academic Press, New York (1980).
37. Kumar, S. and Singh, R. N., "Effect of the Mechanical Boundary Condition at the Crack Surfaces on the Stress Distribution at the Crack Tip in Piezoelectric Materials," *Material Science Engineering: A*, **252**, pp. 64–77 (1998).
38. Lowengrub, M. and Srivastava, K. N., "Two Coplanar Griffith Cracks in an Infinitely Long Elastic Strip," *International Journal of Engineering Science*, **6**, pp. 425–434 (1968).

(Manuscript received April 25, 2013,
accepted for publication January 17, 2014.)

https://doi.org/10.1017/jmech.2014.31 Published online by Cambridge University Press